Proceeding of the IEEE
International Conference on Robotics and Biomimetics
Dali, China, December 2019

Joint Torque Estimation for Dynamic Jumping Control of Compliant Gear-Driven Legged Robot*

Dingan Cheng[1,4], Bingchen Jin[1,2], Caiming Sun[1,2,3,a)], Aidong Zhang[1,2,3] , Shoubin Liu[4]
[1]*Institute of Robotics and Intelligent Manufacturing (IRIM), the Chinese University of Hong Kong (CUHK), Shenzhen, China*
[2]*Shenzhen Institute of Artificial Intelligence and Robotics for Society (AIRS), Shenzhen, China*
[3]*Robotics Research Center, Peng Cheng Laboratory, Shenzhen, China*
[4]*School of Mechanical Engineering and Automation, Harbin Institute of Technology, Shenzhen, China*
[a)]Corresponding Author: Dr. Caiming Sun, cmsun@cuhk.edu.cn

***Abstract* - This paper is to explain compliant torque control for gear driven legged robot. In this paper, active torque compliance control is realized without torque sensor or any mechanically elastic component. The joint torque estimation is very important for torque control. However, Joint torque sensor for medium-size legged robot is so large and heavy that it increases the inertia of the leg, slows down the dynamic response, and leads to complicated electrical system. Therefore, we only use the encoder information and the motor current to estimate the joint torque without torque sensors. Compliant torque control have advantages of absorbing impacts and saving energy. But, torque control is difficult to guarantee the position precision, because the accurate model of the robot is hard to obtain. In order to ensure both compliance and position accuracy, hybrid torque and position control is applied to our robot. In the jumping motion experiments, it is verified that the joint torque can reach peck value in 4.75 ms when jumping up. While The landing peak torque in hybrid control is lower than 1/6 of that under position control and 1/2 of that in torque control. This indicates that the compliance torque control can absorb a large part of shock.**

Index Terms - Legged robot, Compliance control, Dynamic control.

I. INTRODUCTION

Legged robots have powerful motion ability and are able to overcome challenging terrain. When the legged robot is walking, trotting or jumping, its feet would strike the ground and lift periodically [1]. The velocity of the foot end in the vertical direction when striking the ground will cause collision and shock [2]. So the appropriate elasticity on legs is expected to absorb shock and make the robot run more efficient. One approach applied in some famous quadruped robot is to use a kind of actuator named Series Elastic Actuator(SEA), such as StarlETH [3] and ANYmal [4]. The performance of SEA has been showed in these achievements which are verified to be very powerful and effective in quadruped robotics. However, SEA used a mechanical component to form elasticity and passive compliance control [5], which is difficult to precisely control the motion of the leg. What's more, the stiffness of the joint is usually fixed by mechanical component which results in difficulty of interacting with various complicated environments. And the stiffness of the leg is relatively hard to control or change. Different from the passive compliance, another approach used for legged robot to absorb shock and mitigate the collision is active compliance control [6-8] which could make the leg perform as a virtual spring with a damp. The most important advantage of active compliance over the passive compliance is that we can modify the stiffness and damping coefficient in runtime to change the motion performance of the leg. We hope the leg have the low stiffness when is being pushed down and toughing the ground to mitigate the impact. On the other hand, high stiffness is preferred when the leg is lifted up in swing phase, because high stiffness can satisfy the requirements for high position accuracy. From another point of view, position control can be considered as a kind of high-stiffness compliance control. Meanwhile, torque control is able to provide a quite wide range of variable stiffness for adaptive application in complex environments [9].

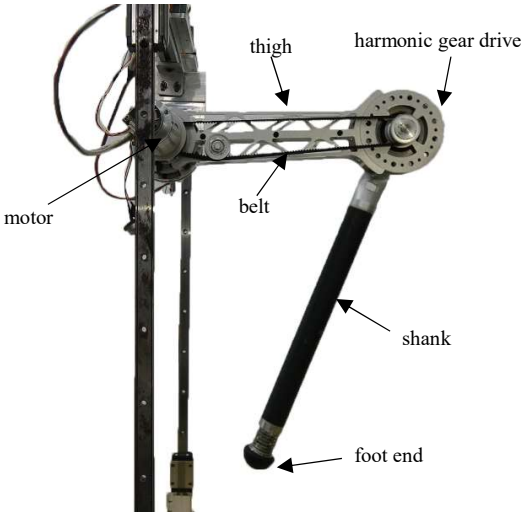

Fig. 1. Two degree of freedom (2-DOF) single leg robot.

For one cycle of jumping actions, there are two connecting motions, named as a stance phase and a swing phase. The jumping height depends on the force value generated by the ground and the reaction time. The quadrupedal animal or biped human keep high position accuracy in the swing phase. When falling down from a high position and the foot end impacting to the ground, they will bend their leg as a buffer. To imitate the real animal, the robot can flex its legs when foot end touching the ground. The straightforward method is to detect the impulses of the joint torque which could indicate the collisions between foot end and the ground. Normally, peak values of the joint torque will appear in a few milliseconds after touching the

* This work is in part supported by the National Natural Science Foundation of China (Grant No. U1613223), in part by the Shenzhen Natural Science Foundation (Grant No. JCYJ20180508163015880), and in part by funding from Shenzhen Institute of Artificial Intelligence and Robotics for Society.

978-1-7281-6321-5/19//$31.00 ©2019 IEEE

ground. So an effective approach is to fast and dynamically regulate the stiffness of legs when foot end touching the ground and lift up alternatively in the stance phase and the swing phase. As one of the most famous and successful quadruped robots, ANYmal's controller has a 90% settling time of 13 ms [4]. In our experiment, the single leg robot can reach its peak torque within 5ms, which enable the robot to response the external impulses fast.

To verify the compliance controller for hybrid position and torque, we use a 2-DOF single leg platform with a hip joint and a knee joint, as shown in Fig. 1. We implement three controllers, position control, torque control, and hybrid position and torque control on it and we compare the actual position and torque trajectory.

This paper is structured as following: The Mechanical and electronic design are described in Section II. Section III provides the joint torque estimation approach for harmonic gear driven actuators. Section IV presents the jumping control of 2-DOF single leg robot based on hybrid position and torque control. Experiments are described in Section V. At last, we conclude in Section VI.

II. Mechanical and Electronic Design for Experiment Platform

In this paper, a single axis platform shown in Fig. 2 is built up for identifying the joint friction model parameters and evaluating the torque estimation. A 2-DOF single leg platform is designed to verify the dynamic and compliant control for the gear-driven actuation based on joint torque estimation.

A. Single axis test platform

The single axis test platform consists of a single joint, a torque sensor and a swinging arm. These three parts are connected by two couplings. The single joint has a harmonic gear driven with reduction ratio of 100 and a high-speed electric motor (Maxon EC45). The output of the harmonic gear is connected to an axis equipped with a torque sensor and a swinging arm. For electrical system, The host control computer with Ubuntu operating system communicates with the motor drive (Elmo Gold Drive) by EtherCAT bus at 1 kHz, and communicates with the torque sensor by serial port at 300 Hz. The EtherCAT master in Ubuntu is based on SOEM (Simple Open EtherCAT Master), an EtherCAT master library writen in C language, which provides powerful interfaces for communicating with the motor drive. The physical model and control diagram of the single axis platform are shown in Fig. 3.

B. Single leg system

The single leg system has two joints, and each joint consists of a high-speed electric motor (Maxon EC45) equipped with a harmonic gear driven with reduction ratio of 100 and a 17 bit absolute encoder. To make the inertia of the robot's leg as small as possible, we would like to simplify the mechanical structure of the leg and place two joint motors upwards, concentrically to the center of mass (CoM) of the whole leg robot. In addition, the knee joint is driven by a motor equipped on hip through a 852 mm total long rubber belt which is used to transmit motor's torque to the harmonic gear on knee joint. The length of the

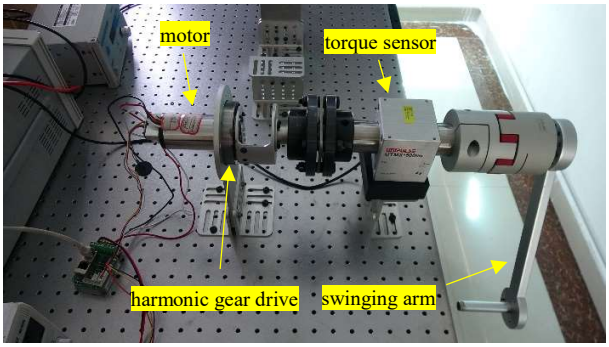

Fig. 2. Single axis test platform.

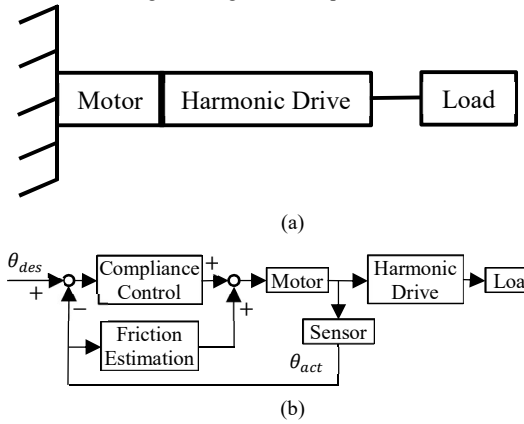

Fig. 3. (a) Physical model of the single axis test platform, (b) Control digram of the single axis test platform.

thigh of this single leg system is 260 mm and the shank length is 422 mm. Relying on the sliding rail, the single leg robot can move back and forth, up and down. The high-reduction gear and the rubber belt can effectively prevent leg shocks on the ground from back driving the upwards knee motor (as shown in Fig. 4). Different from the single axis test platform, the single leg system uses a computer with Windows operating system as the EtherCAT master. The EtherCAT master in Windows is based on TwinCAT and runs at 4 kHz.

III. Joint Torque Estimation

In order to realize the active joint torque control, an accurate joint torque output estimator is required to continuously regulate the motor rotor. In this paper, we accurately correlate the motor currents and encoder readout with the joint torque output and make an estimation of the joint torque for the fast and dynamic jumping control of compliant gear-driven legged robots.

A. Dynamics of the single leg robot

The lagrange motion equation of the single leg is:

$$\boldsymbol{\tau} + \boldsymbol{J}^{\boldsymbol{T}}(\boldsymbol{q})\boldsymbol{f} = \boldsymbol{M}(\boldsymbol{q})\ddot{\boldsymbol{q}} + \boldsymbol{V}(\boldsymbol{q}, \dot{\boldsymbol{q}}) + \boldsymbol{G}(\boldsymbol{q}) \qquad (1)$$

where $\boldsymbol{\tau}$ is the joint torque vector, $\boldsymbol{J}^{\boldsymbol{T}}(\boldsymbol{q})$ is the transposition of the Jacobian matrix, $\boldsymbol{f}$ is the external force applied on the foot end. $\boldsymbol{M}(\boldsymbol{q})$ is the inertia matrix, $\boldsymbol{V}(\boldsymbol{q}, \dot{\boldsymbol{q}})$ is the centrifugal and Coriolis force, and $\boldsymbol{G}(\boldsymbol{q})$ is the gravity of the leg.

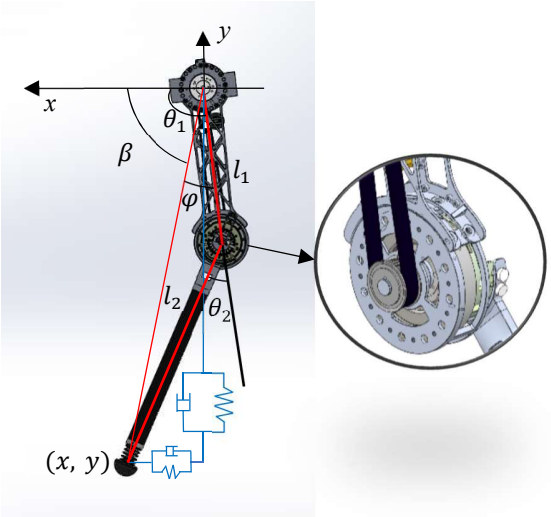

Fig. 4. Structure of the single leg system and the knee joint.

Apply the lagrange motion equation to our single leg platform, the motion equation can be obtained:

$$\tau_i + R_i I_{rotor}\ddot{\theta}_{rotor} + \tau_{friction}^{(i)} = R_i \tau_{motor}^{(i)} \quad (2)$$

where τ_i is the *i*th row of the joint output torque vector. R_i is the reduction ratio of the *i*th joint. I_{rotor} is the inertia of the rotor and the wave generator. Because the rotor and the wave generator are fixed, they could be considered as a whole body. $\tau_{friction}^{(i)}$ is the friction torque mainly in the harmonic gear. $\tau_{motor}^{(i)}$ is the output torque of the motor. For single joint, omitting the index *i*, we can obtain the joint torque formula as follow:

$$\tau = R\tau_{motor} - RI_{rotor}\ddot{\theta}_{rotor} - \tau_{friction} \quad (3)$$

B. Joint torque estimation

Friction behaviour on robot joint with high-reduction gear is extremely complicated which is nonlinear and multidimensional. There isn't perfect theory for the complicated friction behaviour. However, there are some feasible friction model used for approximating the friction force or torque value, such as Coulomb model, viscous model, Stribeck model, LuGre model [10] and so on [11-13]. A simple but effective model can simplify the calculation and provide reliable accuracy. For example, Coulomb + viscous model was a simplified and effective model verified in [14]. In Ref [15], we have made an accurate and nonlinear model on gear-driven joint for low-speed motors (Maxon EC 90 flat).

In our robot, it is found that the velocity have little effects on friction torque value for high-speed motor Maxon EC 45, as shown in Fig. 5. So, to simplify the calculation, the model can be further simplified to Coulomb friction. So, the joint friction torque value can be obtained by the following formula:

$$\tau_{friction} = c\ sgn(\dot{\theta}) \quad (4)$$

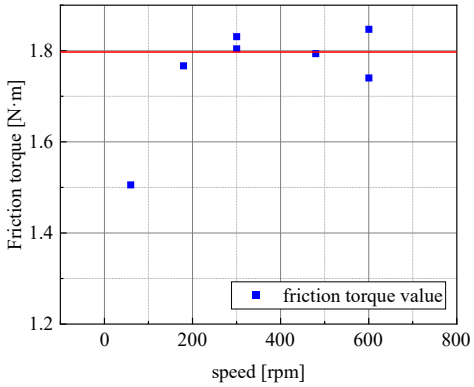

Fig. 5. Friction tested value at various angular velocity.

where c is a constant, $\dot{\theta}$ is the joint angular velocity, and sgn(·) is the Sign function. Its return value is given by (5).

$$sgn(x) = \begin{cases} 1, & x \geq 0 \\ -1, & x < 0 \end{cases} \quad (5)$$

We have measured the friction at several speed and several times. Average the result, we obtain c = 1.79 Nm. In order to evaluate the accuracy of the friction torque estimation, we drag the swinging arm by hand and record the estimated torque value and the sensed torque value as shown in Fig. 6.

IV. Hybrid Position and Torque Control

In order to make torque-controlled actuators excellently operate on the legged robot, a hybrid position and torque control is implemented according to the requirements for position accuracy or force compliance at different phases of locomotion. In torque compliance control, we use joint torque estimation to provide virtual feedbacks on each joint and form the compliance for the whole leg. In position control, a high-gain position control loop is used to provide high position accuracy. Close loop control for position and torque is processed on the Elmo Gold Drive. Host computer would generate the trajectory and provide the target position by every control loop via EtherCAT bus. The control strategy implemented in the motor drive could guarantee better position accuracy, and run at much higher frequency, which will be verified later in Section V.

A. Torque compliance control

In (3), the joint output torque vector $\boldsymbol{\tau}$ consists two parts: $\boldsymbol{\tau}_{gravity}$ and $\boldsymbol{\tau}_{motion}$. Since $RI_{rotor}\ddot{\theta}_{rotor} \ll \tau_{friction}$, we can turn (3) to:

$$\boldsymbol{\tau}_{motor} = \left(\boldsymbol{\tau}_{motion} + \boldsymbol{\tau}_{friction} + \boldsymbol{\tau}_{gravity}\right)/R \quad (6)$$

where $\boldsymbol{\tau}_{motion}$ is the joint torque vector required for making the leg compliant as a virtual spring-damper system, as shown in Fig. 4, $\boldsymbol{\tau}_{motion}$ can be calculated by (7), $\boldsymbol{\tau}_{friction}$ is the friction torque vector, and $\boldsymbol{\tau}_{gravity}$ is the torque vector required for cpmpensating the gravity.

$$\boldsymbol{\tau}_{motion} = \boldsymbol{J}^T\left(G_P\boldsymbol{P}_{err} + G_D\dot{\boldsymbol{P}}_{act}\right) \quad (7)$$

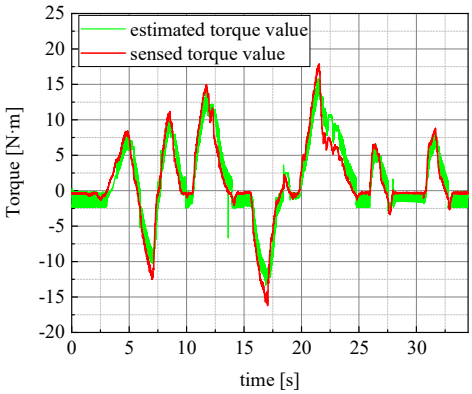

Fig. 6. Joint torque estimated value and sensed value on the single axis platform.

where $\boldsymbol{J^T}$ is the tansposition of the Jacobian matrix, $\boldsymbol{P}_{err}$ is the position error vector of foot end which can be calculated by (8), G_P and G_D are the spring coefficient and damper coefficient.

$$\boldsymbol{P}_{err} = \boldsymbol{P}_{des} - \boldsymbol{P}_{act} \tag{8}$$

where $\boldsymbol{P}_{des}$ is desired foot end position. To eliminate the gravity effect, there should be addition torque $\boldsymbol{\tau}_{gravity}$ used to compensate gravity:

$$\boldsymbol{\tau}_{gravity} = \begin{bmatrix} m_1 g l_{c1} cos\theta_1 + m_2 g l_1 cos\theta_1 + m_2 g l_{c2} \cos(\theta_1 - \theta_2) \\ m_2 g l_{c2} \cos(\theta_1 - \theta_2) \end{bmatrix} \tag{9}$$

where m_1, m_2 are the mass of thigh and shank, g is the gravity acceleration, l_1 is the length of thigh link, l_{c1} is the distance from the center of mass of thigh link to hip joint rotation center, l_{c2} is the distance from the center of mass of shank link to the knee joint rotation center, and θ_1, θ_2 are the joint angular of hip and knee which are marked in Fig. 4.

Using the geometry of the single leg robot, we can obtain the coordinate of the foot end:

$$\boldsymbol{P} = \begin{bmatrix} x \\ y \end{bmatrix} = \begin{bmatrix} l_1 cos\theta_1 + l_2 cos(\theta_1 - \theta_2) \\ -l_1 sin\theta_1 - l_2 sin(\theta_1 - \theta_2) \end{bmatrix} \tag{10}$$

By geometric method, the inverse kinematics can be presented as following:

$$\boldsymbol{\theta} = \begin{bmatrix} \theta_1 \\ \theta_2 \end{bmatrix} = \begin{bmatrix} \beta + \varphi \\ \pi - \arccos\left(\frac{l_1^2 + l_2^2 - x^2 - y^2}{2 l_1 l_2}\right) \end{bmatrix} \tag{11}$$

where β and φ satisfy (12) and (13):

$$\beta = \frac{\pi}{2} + \arctan\frac{x}{y} \tag{12}$$

$$\varphi = \arccos\frac{l_1^2 + x^2 + y^2 - l_2^2}{2 l_1 \sqrt{x^2 + y^2}} \tag{13}$$

The control diagram of the torque compliance control and position control we used is shown in Fig. 7.

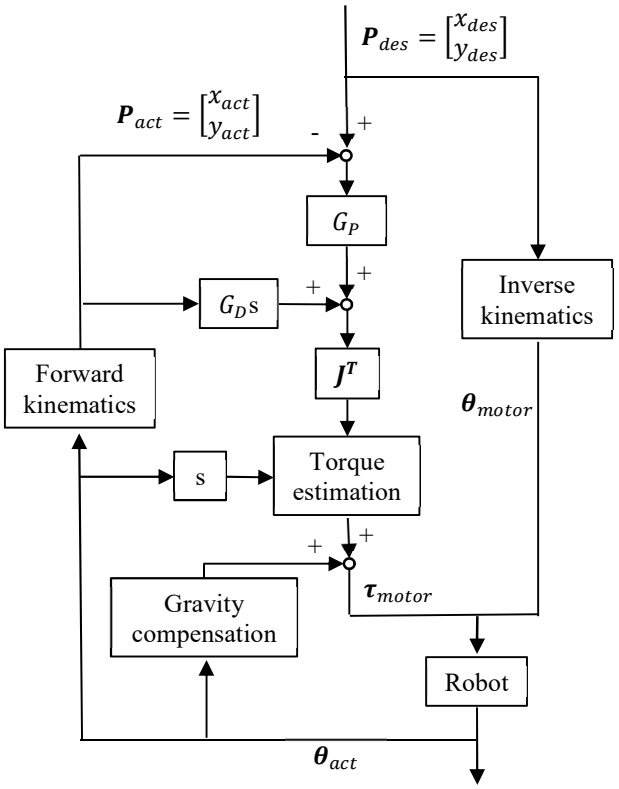

Fig. 7. Control diagram of the single leg system.

B. *Hybrid position and torque control*

If high-gain position control is applied to the robot all the time, joint torque values will become quite high impulses when its foot end striking the ground. During leg jumping, the flexion of the leg when touching the ground is not allowed for position control, the peak torque on the joint is even higher. This will be shown later in Section V. In fact, real animals are able to flex their legs a little bit to buffer the kinetic energy of falling down and prolong the deceleration time. A simple method to imitate real biology is to use torque compliance control proposed above and form virtual elastics on the whole leg. External impacts applied to the leg could result in a displacement of the foot end. We can regulate the stiffness of the virtual spring to extend the displacement which will reduce the peak joint torque value.

C. *Trajectory generator*

During jumping of legged robots, the trajectory of foot end has important influence on stability of the motion control. A stable trajectory must not only satisfy the continuity of the first derivative but also satisfy the continuity of the second derivative. This could avoid impacts when foot ends interact with complicated environments. Bezier curve has greater flexibility than interpolating curve. Given an ordered set of points as control points, we can use the Bezier curve to approximate the points trajectory, and this curve only passes through the first point and the last point. A Bezier curve of

degree n, controlled by $n + 1$ points, can be represented as a parametric function of following form:

$$Q(t) = \sum_{i=0}^{n} V_i B_{i,n}(t), t \in [0,1] \quad (14)$$

where V_i is the point coordinate vector and $B_{i,n}(t)$ is called the Bernstein polynomials calculated by (15).

$$B_{i,n}(t) = C_n^i t^i (1-t)^{n-i}, t \in [0,1] \quad (15)$$

where C_n^i is the binomial coefficient which can be represented as $C_n^i = \frac{n!}{i!(n-i)!}$.Bezier curve has good flexibility and continuity which could be connected to other curve easily and smoothly. So, we design the trajectory generator based on Bezier curves.

V. Experiments

A. *Tracking experiments of foot end under torque compliance control*

The torque compliance control makes the robot's legs perform as a virtual spring to absorb shock and buffer kinetic energy. Considering the robotic legs as massless legs, a spring-damper system can be used to model the whole leg, as shown in Fig. 4. An external force applied to the foot end will make a displacement to a point where the joint torque keeps equilibrium with the external force. When this external force is released, the foot end will return the original point with some displacement errors after the vibration is attenuated to nearly zero. Furthermore, if the friction is taken into consideration, the motors are also able to build up equilibrium with external forces. Under accurate torque estimation, as the external force is released, the foot end is able to return its original point with less displacement error. It can demonstrate the good tracking

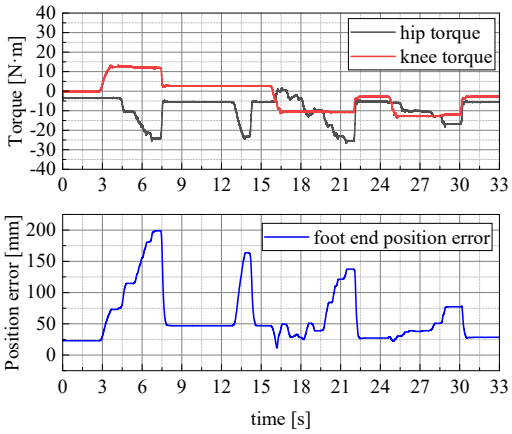

Fig. 8. The foot end position error when the foot is pulled and released without friction compensation and torque of hip joint and knee joint.

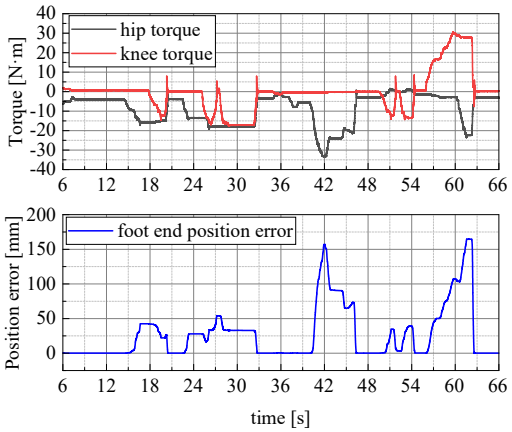

Fig. 9. The foot end position error when the foot is pulled and released with friction compensation and torque response of hip joint and knee joint.

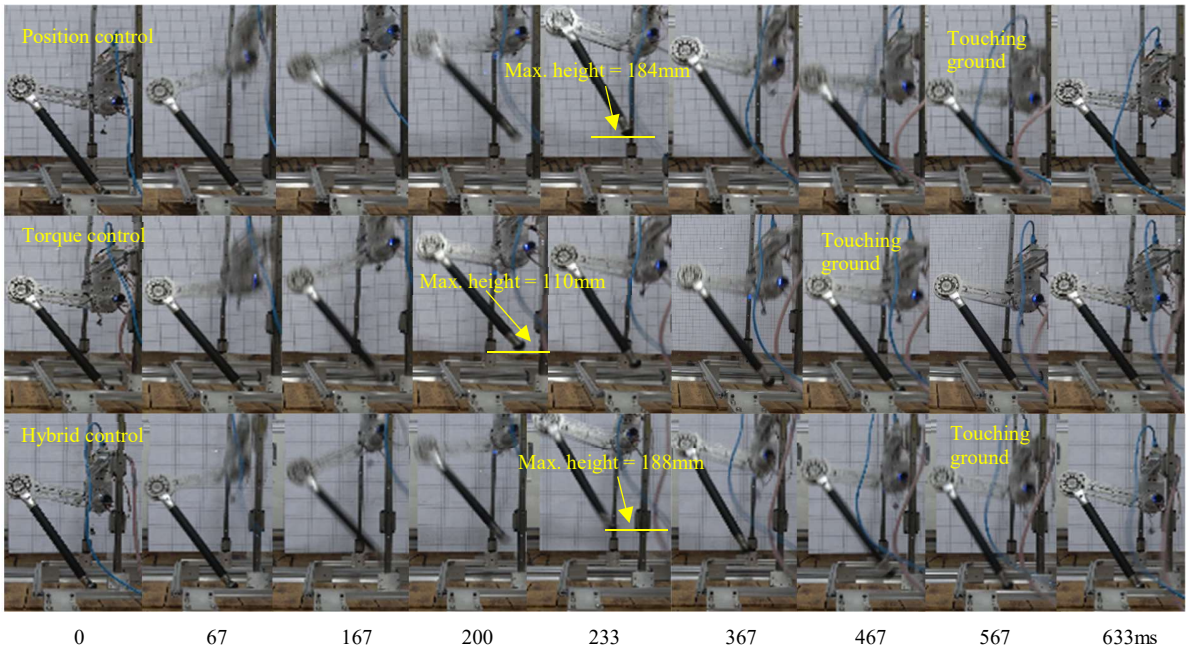

Fig. 10. The single leg robot jumped under position control, torque control and hybrid control.

performance of foot end under torque compliance control of the whole leg.

According to these properties, we design an experiment to check if the foot end is able to return original point after disturbance by external forces. This tracking results could be used to verify if both torque and position accuracy are maintained under torque compliance control. If the estimated friction torque is not accurate enough, the leg will keep vibrating around the original point, or the foot end cannot return its original point.

In the experiments, the leg is pushed and pulled under external force, the foot end is forced to leave from the original position and returns after external force released. As shown in Fig. 8 and Fig. 9, the position error of foot end is below 1 mm after the leg is released under accurate torque estimation with friction compensation. Without friction compensation, the errors increases to 23 mm ~ 46 mm. This indicates that the friction compensation is relatively effective and the torque estimation is quite accurate.

B. Jumping experiments

Joint torque estimation can provide accurate motion control which can ensure stationarity when switching the control modes. Based on these motion control strategies, we implement the jumping motion of the robot.

The foot end trajectory in jumping motion is simplified to a Bezier curve controlled by seven points. Fig. 10 shows the jumping motion. Using 7 points Bezier curve, we can implement decoupled control of jumping height and forward step distance. The jumping height depend on the y coordinate values of the control points, and the forward step distance is affected by the x coordinate values. In our experiments, we set all the x coordinate values to zero to avoid the robot's forth-back movement. The leg jumping consists of following procedures: First, the robot stand up and keep the posture preparing for jumping. Secondly, the robot extends its leg and lift up the body in only 0.1 second. The robot has been flying in the air at this time. Third, the robot spends another 0.1 second flexing its leg to prepare for landing. Last, the robot land and return the initial posture for next jumping.

We have designed three groups of experiments using hybrid position and torque control, torque control and high-gain position control. Given the same foot end trajectory in each group, the robot started jumping at 0 milliseconds. The jumping heights are 184 mm under position control, 110 mm under torque control and 188 mm under hybrid control. As shown in Fig. 11 and Fig. 12, the touching ground time is 550 ms under position control, 460 ms under torque control, and 576 ms under hybrid control. The time of touching ground indicates the jumping height which could indicates the position accuracy when jumping up.

Firstly, in position control experiment, the robot achieves peak torque value of 162.72 Nm in knee joint at 4.75 milliseconds. As shown in Fig. 11 and Fig. 12, the position control could follow the desired position accurately. The peak torques when jumping are 151.84 Nm in hip joint and 162.72 Nm in knee joint. The torque value in hip joint did not vary obviously when landing. The peak value of actual y coordinate

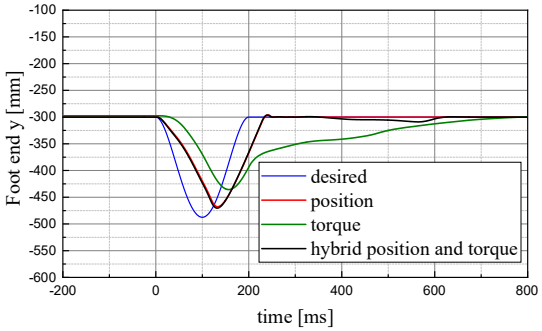

Fig. 11. The y coordinate value of desired foot end position and actual foot end position in three groups of jumping motion experiments.

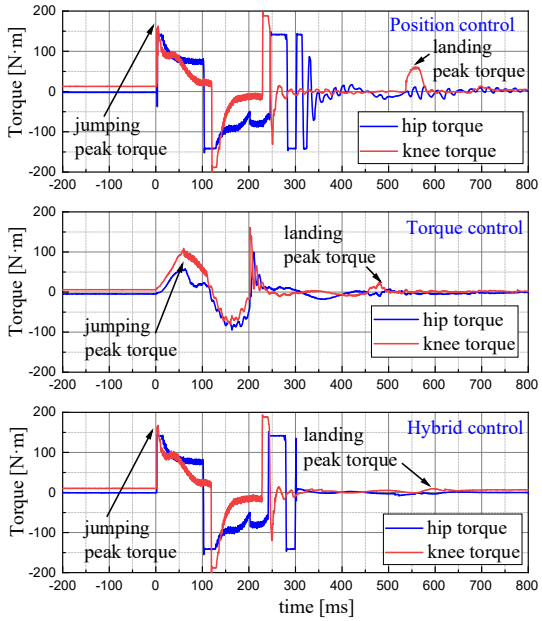

Fig. 12. Joint torque value in jumping motion under position control, torque control and hybrid control.

of foot end position lags behind the desired peak value about 32 milliseconds. But, the landing peak torque value achieved 61.58 Nm which is higher than the 1/3 of jumping peak value. Because, under high-gain position control, the motor drive generates a high torque when the foot end strikes the ground. This is inefficient and may damage the system and mechanical parts.

Secondly, in torque control experiment, the jumping peak torques are 57.98 Nm in hip joint and 107.84 Nm in knee joint and the landing peak torque in knee joint is 24.21 Nm. The foot end arrived at the furthest point after a latency of 58 ms which is almost as twice as one under position control. In addition, greaterposition tracking error makes the jumping lower than position control. However, torque control provides good compliance for the whole leg, and the peak torque values during landing are much lower than those under position control.

At last, Hybrid position and torque control delivers both highly dynamic response with good position accuracy and force compliance, as shown in Fig. 11 and Fig. 12. The y coordinate variation curves of foot end coincide with those under position

control from 0 ms to 350 ms. The jumping peak torques are 145.42 Nm in hip joint and 164.74 Nm in knee joint, and the landing peak torque is only 9.46 Nm.

In these three groups of experiments, all the landing torque response of hip joint are not remarkable, because the direction of impact force passes through the hip joint rotation axis. Large leg inertia leads to the second peak torque value, because shank and thigh should decelerate to static pose within below 100 ms. Under hybrid position and torque control, the landing peak torques are lower than those in torque control, because the position error is smaller as a result of position control before landing.

VI. Conclusion

As shown in the experiments, the joint torque could rise to peak value in only 5 milliseconds. Leg's virtual stiffness could vary highly dynamically in fast adaption of complicated environment and the difficulty of quick action for large-inertia leg.

References

[1] Zeng, Ganwen , and A. Hemami . *An overview of robot force control*. Cambridge University Press, 1997.

[2] Englsberger, Johannes, et al. "Overview of the torque-controlled humanoid robot TORO." *2014 IEEE-RAS International Conference on Humanoid Robots*. IEEE, 2014.

[3] Hutter, Marco, et al. "StarlETH: A compliant quadrupedal robot for fast, efficient, and versatile locomotion." *Adaptive Mobile Robotics*. 2012. 483-490.

[4] Hutter, Marco, et al. "Anymal-a highly mobile and dynamic quadrupedal robot." *2016 IEEE/RSJ International Conference on Intelligent Robots and Systems (IROS)*. IEEE, 2016.

[5] M. Hutter, C. D. Remy, M. A. Hoepflinger, and R. Siegwart, "Efficient and Versatile Locomotion With Highly Compliant Legs," *IEEE/ASME Trans. Mechatron.*, vol. 18, no. 2, pp. 449–458, Apr. 2013.

[6] A. Calanca, R. Muradore, and P. Fiorini, "A Review of Algorithms for Compliant Control of Stiff and Fixed-Compliance Robots," *IEEE/ASME Trans. Mechatron.*, vol. 21, no. 2, pp. 613–624, Apr. 2016.

[7] Jin, Bingchen, et al. "Single leg compliance control for quadruped robots." *Proceedings - 2017 Chinese Automation Congress (CAC),* Pages: 7624-7628, Jinan, China, 20-22 Oct. 2017.

[8] Boaventura, Thiago, et al. "Dynamic torque control of a hydraulic quadruped robot." *2012 IEEE international conference on robotics and automation*. IEEE, 2012.

[9] S.-H. Hyon, D. Suewaka, Y. Torii, and N. Oku, "Design and Experimental Evaluation of a Fast Torque-Controlled Hydraulic Humanoid Robot," *IEEE/ASME Trans. Mechatron.*, vol. 22, no. 2, pp. 623–634, Apr. 2017.

[10] Gandhi, Prasanna S., Fathi H. Ghorbel, and James Dabney. "Modeling, identification, and compensation of friction in harmonic drives." *Proceedings of the 41st IEEE Conference on Decision and Control, 2002.*. Vol. 1. IEEE, 2002.

[11] Taghirad, H. D., and P. R. Belanger. "An experimental study on modelling and identification of harmonic drive systems." *Proceedings of 35th IEEE Conference on Decision and Control*. Vol. 4. IEEE, 1996.

[12] Lu, Yu-Sheng, and Chi-Sheng Hwang. "Tracking control of a harmonic drive actuator with sliding-mode disturbance observers." *2009 IEEE/ASME International Conference on Advanced Intelligent Mechatronics*. IEEE, 2009.

[13] T. D. Tuttle and W. P. Seering, "A nonlinear model of a harmonic drive gear transmission," *IEEE Trans. Robot. Automat.*, vol. 12, no. 3, pp. 368–374, Jun. 1996.

[14] Nagamatsu, Yuya, et al. "Distributed torque estimation toward low-latency variable stiffness control for gear-driven torque sensorless humanoid." *2017 IEEE/RSJ International Conference on Intelligent Robots and Systems (IROS)*. IEEE, 2017.

[15] Bingchen Jin, Caiming Sun, Aidong Zhang, et al., "Joint Torque Estimation toward Dynamic and Compliant Control for Gear-Driven Torque Sensorless Quadruped Robot," in *IEEE/RSJ International Conference on Intelligent Robots and Systems(IROS) 2019*, Nov 2019.